2020 American Control Conference
Denver, CO, USA, July 1-3, 2020

A Time-Delayed Lur'e Model with Biased Self-Excited Oscillations

Juan Paredes, Syed Aseem Ul Islam, and Dennis S. Bernstein

***Abstract*— Self-excited systems arise in many applications, such as biochemical systems, mechanical systems with fluid-structure interaction, and fuel-driven systems with combustion dynamics. This paper presents a Lur'e model that exhibits biased oscillations under constant inputs. The model involves arbitrary asymptotically stable linear dynamics, time delay, a washout filter, and a saturation nonlinearity. For all sufficiently large scalings of the loop transfer function, these components cause divergence under small signal levels and decay under large signal amplitudes, thus producing an oscillatory response. A bias-generation mechanism is used to specify the mean of the oscillation. The main contribution of the paper is the presentation and analysis of a discrete-time version of this model.**

I. Introduction

A self-excited system has the property that the input is constant but the response is oscillatory. Self-excited systems arise in numerous applications, such as biochemical systems, fluid-structure interaction, and combustion. The classical example of a self-excited system is the van der Pol oscillator, which has two states whose asymptotic response converges to a limit cycle. A self-excited system, however, may have an arbitrary number of states and need not possess a limit cycle. Overviews of self-excited systems are given in [1], [2], and applications to chemical and biochemical systems are discussed in [3]–[5]. Self-excited thermoacoustic oscillation in combustors is discussed in [6], [7].

Models of self-excited systems are typically derived in terms of the relevant physics of the application. From a systems perspective, the main interest is in understanding the features of the components of the system that give rise to self-sustained oscillations. Understanding these mechanisms can illuminate the relevant physics in specific domains and provide unity across various domains.

A unifying model for self-excited systems is a feedback loop involving linear and nonlinear elements; systems of this type are called *Lur'e systems*. Lur'e systems have been widely studied in the classical literature on stability theory [8]. Within the context of self-excited systems, Lur'e systems under various assumptions are considered in [2], [9]–[15]. Application to thermoacoustic oscillation in combustors is considered in [16]. Self-oscillating discrete-time systems are considered in [17]–[20].

Roughly speaking, self-excited oscillations arise from a combination of stabilizing and destabilizing effects. Destabilization at small signal levels causes the response to grow from the vicinity of an equilibrium, whereas stabilization at large signal levels causes the response to decay from large signal levels. In particular, negative damping at low signal levels and positive damping at high signal levels is the mechanism that gives rise to a limit cycle in the van der Pol oscillator. Note that, although systems with limit-cycle oscillations are self-excited, the converse need not be true since the response of a self-excited system may oscillate without the trajectory reaching a limit cycle. Alternative mechanisms exist, however; for example, time delays are destabilizing, and Lur'e models with time delay have been extensively considered as models of self-excited systems [21].

The present paper considers a time-delayed Lur'e (TDL) model that exhibits self-excited oscillations. This model, which is illustrated in Figure 1, incorporates the following components:

- $i)$ Asymptotically stable linear dynamics.
- $ii)$ Time delay.
- $iii)$ A washout (that is, highpass) filter.
- $iv)$ A continuous, bounded nonlinearity $\mathcal{N}\colon \mathbb{R} \to \mathbb{R}$ that satisfies $\mathcal{N}(0) = 0$, is either nondecreasing or nonincreasing, and changes sign (positive to negative or vice versa) at the origin.
- $v)$ A bias-generation mechanism, which produces an offset in the oscillatory response that depends on the value of the constant external input.

A notable feature of this model is that self-oscillations are guaranteed to exist for arbitrary asymptotically stable dynamics, in contrast to [22], where the dynamics are assumed to be passive. We note that washout filters are used in [23] to achieve stabilization, whereas, in the present paper, they are used to create self-oscillations.

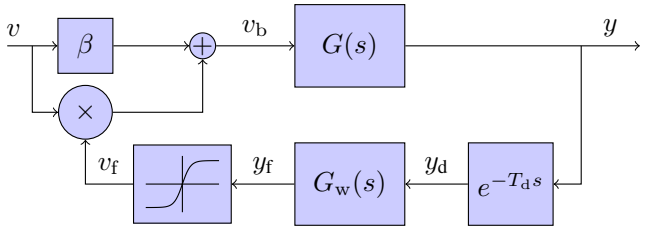

Fig. 1: Continuous-time, time-delayed Lur'e model with constant input u and bias generation.

For this time-delay Lur'e model, the time-delay provides the destabilization mechanism, while, under large signal levels, the saturation function yields a constant signal, which effectively breaks the loop, thus allowing the open-loop dynamics to stabilize the response. This stabilization occurs at large amplitude. In order to create an oscillatory response,

Juan Paredes, Syed Aseem Ul Islam, and Dennis S. Bernstein are with the Department of Aerospace Engineering, University of Michigan, Ann Arbor, MI, USA. {jparedes, aseemisl, dsbaero}@umich.edu

the Lur'e model includes a washout filter, which removes the DC component of the delayed signal $y_{\rm d}$ and allows the saturation function to operate in its small-signal linear region. A similar feature appears in [2], [9]–[12] in the form of the numerator s in G for the case where y represents velocity. This combination of elements produces self-excited oscillations for all sufficiently large scalings of the asymptotically stable dynamics. An additional feature of this model is the ability to produce oscillations with a bias, that is, an offset. This is done by the bias-generation mechanism involving the scalar β.

The analysis and examples in the paper focus on a discrete-time version of the time-delayed Lur'e model with the standard saturation function. This setting simplifies the analysis of solutions as well as the numerical simulations. Proofs of all results in this paper are omitted due to limited space.

II. Time-Delayed Linear Feedback model

In this section we consider the discrete-time, time-delayed Lur'e model shown in Figure 2, where α is a real number, G is a strictly proper SISO transfer function, $G_d(z) \triangleq 1/z^d$ is a d-step delay, where $d \geq 0$, and $G_{\rm w}(z) \triangleq (z-1)/z$ is a washout, that is, highpass, filter. Let $G = N/D$, where the polynomials N and D are coprime, D is monic, $n \triangleq \deg D$, and $m \triangleq \deg N$.

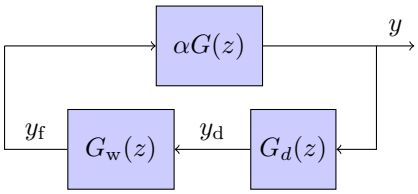

Fig. 2: Discrete-time time-delayed linear feedback system.

Let $(A, B, C, 0)$ be a minimal realization of G whose internal state at step k is $x_k \in \mathbb{R}^n$. Furthermore, consider the realization $(N_{\rm d}, e_{{\rm d},d}, e_{1,d}^{\rm T}, 0)$ of G_d with internal state $x_{{\rm d},k} \in \mathbb{R}^d$, where $N_{\rm d}$ is the standard $d \times d$ nilpotent matrix and $e_{i,d}$ is the ith column of the $d \times d$ identity matrix I_d. Finally, let $(0, 1, -1, 1)$ be a realization of $G_{\rm w}$ with internal state $x_{\rm w} \in \mathbb{R}$, and let α be a real number that scales G. Then, the discrete-time, time-delayed linear feedback model shown in Figure 2 has the closed-loop dynamics

$$\begin{bmatrix} x_{k+1} \\ x_{{\rm d},k+1} \\ x_{{\rm w},k+1} \end{bmatrix} = \begin{bmatrix} A & \alpha B e_{1,d}^{\rm T} & -\alpha B \\ e_{d,d} C & N_d & 0 \\ 0 & e_{1,d}^{\rm T} & 0 \end{bmatrix} \begin{bmatrix} x_k \\ x_{{\rm d},k} \\ x_{{\rm w},k} \end{bmatrix}, \quad (1)$$

with output

$$y_k = \begin{bmatrix} C & 0 & 0 \end{bmatrix} \begin{bmatrix} x_k \\ x_{{\rm d},k} \\ x_{{\rm w},k} \end{bmatrix} \quad (2)$$

and internal signals

$$y_{{\rm d},k} = e_{1,d}^{\rm T} x_{{\rm d},k}, \quad (3)$$

$$y_{{\rm f},k} = -x_{{\rm w},k} + y_{{\rm d},k}. \quad (4)$$

For all $d \geq 0$, define $L_d \triangleq G G_{\rm w} G_d$. Finally, for all $d \geq 0$ and $\alpha \in \mathbb{R}$, the characteristic polynomial $p_{d,\alpha}$ of the closed-loop model is given by

$$p_{d,\alpha}(z) \triangleq z^{d+1} D(z) - \alpha(z-1) N(z). \quad (5)$$

Note that, for all $\alpha \in \mathbb{R}$, 1 is not a root of $p_{d,\alpha}$.

The following result consists of two statements. The first statement shows that, for sufficiently large values of the delay d, the Nyquist plot of L_d unfolds clockwise, while the second statement shows that the linear closed-loop system is asymptotically stable only for values of α contained in a bounded interval.

Theorem 2.1: The following statements hold:

i) There exists $\bar{d} \geq 0$ such that, for all $\theta \in [0, \pi]$ and all $d > \bar{d}$,

$$\frac{\rm d}{{\rm d}\theta} \angle L_d(e^{\jmath\theta}) < 0. \quad (6)$$

ii) There exists $\bar{d} \geq 0$ such that, for all $d > \bar{d}$, there exist $\alpha_{d,{\rm l}} < 0$ and $\alpha_{d,{\rm u}} > 0$ such that $p_{d,\alpha}$ is asymptotically stable if and only if $\alpha \in (\alpha_{d,{\rm l}}, \alpha_{d,{\rm u}})$.

The numerical results in this section suggest that

$$\alpha_\infty \triangleq \lim_{d\to\infty} -\alpha_{d,{\rm l}} = \lim_{d\to\infty} \alpha_{d,{\rm u}} > 0, \quad (7)$$

which in turn implies that the minimum magnitude of α required for destabilizing the model converges to a single value as d increases. A proof of this statement will be pursued in future work.

Let $z = e^{\jmath\theta} \neq 1$, where $\theta \in (0, \pi]$, be a root of $p_{d,\alpha}$ on the unit circle. The corresponding value $\alpha(\theta)$ of α is given by

$$\alpha(\theta) = \frac{e^{\jmath(d+1)\theta}}{(e^{\jmath\theta} - 1) G(e^{\jmath\theta})}. \quad (8)$$

Note that

$$\alpha(\theta) = \frac{[(\cos d\theta - \cos(d+1)\theta) + \jmath(\sin d\theta - \sin(d+1)\theta)] G^{-1}(e^{\jmath\theta})}{2 - 2\cos(\theta)}. \quad (9)$$

Writing $G^{-1}(e^{\jmath\theta}) = a(\theta) + \jmath b(\theta)$, it follows that

$$\alpha(\theta) = \frac{f(\theta) + \jmath g(\theta)}{2 - 2\cos\theta}, \quad (10)$$

where

$$f(\theta) \triangleq a(\theta)[\cos d\theta - \cos(d+1)\theta] - b(\theta)[\sin d\theta - \sin(d+1)\theta], \quad (11)$$

$$g(\theta) \triangleq b(\theta)[\cos d\theta - \cos(d+1)\theta] + a(\theta)[\sin d\theta - \sin(d+1)\theta]. \quad (12)$$

Note that $\alpha(\theta)$ is real if and only if $g(\theta) = 0$. In fact, the values of θ that satisfy $g(\theta) = 0$ are the angles for which at least one root of $p_{d,\alpha}$ lie on the unit circle for a given value

of d and for the corresponding real value $\alpha = \alpha(\theta)$. Note that $g(\theta) = 0$ if and only if

$$b(\theta) = -a(\theta)\frac{\sin d\theta - \sin(d+1)\theta}{\cos d\theta - \cos(d+1)\theta}, \tag{13}$$

and thus

$$\begin{aligned} f(\theta) &= a(\theta)\frac{[\cos d\theta - \cos(d+1)\theta]^2 + [\sin d\theta - \sin(d+1)\theta]^2}{\cos d\theta - \cos(d+1)\theta} \\ &= a(\theta)\frac{2 - 2\cos d\theta\cos(d+1)\theta - 2\sin d\theta\sin(d+1)\theta}{\cos d\theta - \cos(d+1)\theta} \\ &= a(\theta)\frac{2 - 2\cos\theta}{\cos d\theta - \cos(d+1)\theta}. \end{aligned} \tag{14}$$

Therefore, $\alpha(\theta)$ is given by

$$\alpha(\theta) = \frac{a(\theta)}{\cos d\theta - \cos(d+1)\theta}. \tag{15}$$

Example 2.2: Let $G(z) = \frac{1}{z+p}$, where $p \in (-1, 1)$, and let $z = e^{\jmath\theta} \neq 1$ be a root of $p_{d,\alpha}$ on the unit circle. Then $a(\theta) = \cos\theta + p$, $b(\theta) = \sin\theta$, and (8) and (15) have the form

$$\alpha(\theta) = \frac{e^{\jmath(d+2)\theta} + pe^{\jmath(d+1)\theta}}{e^{\jmath\theta} - 1} = \frac{\cos\theta + p}{\cos d\theta - \cos(d+1)\theta}, \tag{16}$$

which implies that

$$|\alpha(\theta)| = \sqrt{\frac{p^2 + 2p\cos\theta + 1}{2 - 2\cos\theta}}. \tag{17}$$

Furthermore, it follows from (13) that

$$\sin(d+2)\theta = (1-p)\sin(d+1)\theta + p\sin d\theta. \tag{18}$$

Since L_d has $d+2$ poles in the open unit disk and one zero, which is at $z = 1$, it follows that there exist exactly $d+1$ values $\theta_1, \ldots, \theta_{d+1}$ of $\theta \in [0, \pi]$ that satisfy (18). The corresponding values of $\alpha(\theta_i)$ are given by

$$\begin{aligned} \alpha(\theta_i) &= \frac{\cos\theta_i + p}{\cos d\theta_i - \cos(d+1)\theta_i} \\ &= \frac{-\cos(d+2)\theta_i + (1-p)\cos(d+1)\theta_i + p\cos d\theta_i}{2 - 2\cos\theta_i}. \end{aligned} \tag{19}$$

For $p = 0.5$, $d = 6$, and $d = 7$, Figure 3 shows $\alpha(\theta_i)$ and $|\alpha(\theta_i)|$ versus θ_i. Note that, for both values of d, the minimum value of $|\alpha(\theta_i)|$ occurs at $\theta = \pi$. Finally, Figure 4 shows $\alpha_{d,\mathrm{l}}$ and $\alpha_{d,\mathrm{u}}$ versus d for $p = 0.5$, which indicates that $\lim_{d\to\infty} -\alpha_{d,\mathrm{l}} = \lim_{d\to\infty} \alpha_{d,\mathrm{u}}$.

Special case: For $p = 0$, (17) becomes

$$|\alpha(\theta)| = \frac{1}{\sqrt{2 - 2\cos\theta}}, \tag{20}$$

and (18) becomes

$$\sin(d+1)\theta = \sin(d+2)\theta. \tag{21}$$

Note that, for all integers i, $\sin(d+1)\theta = \sin((2i+1)\pi - (d+1)\theta)$. Therefore, (21) holds if and only if $\theta = \frac{2k+1}{2d+3}\pi$. Hence, $\theta \in [0, \pi]$ satisfies (21) if and only if there exists $i \in \{0, \ldots, d+1\}$ such that $\theta_k \triangleq \left(\frac{2i+1}{2d+3}\right)\pi$. For these $d+2$ values of θ, it follows from (19) that the corresponding values of $\alpha(\theta)$ are given by

$$\begin{aligned} \alpha(\theta_i) &= \frac{\cos\theta_i}{\cos d\theta_i - \cos(d+1)\theta_i} \\ &= \frac{\cos(d+1)\theta_i - \cos(d+2)\theta_i}{2 - 2\cos\theta_i}. \end{aligned} \tag{22}$$

Next, it can be shown that, for all $i \in \{1, \ldots, d\}$, $\alpha(\theta_i)\alpha(\theta_{i+1}) < 0$. Note that $\theta_{d+1} = \pi$ and $\alpha(\theta_{d+1}) = (-1)^{d+1}0.5$. Hence, $|\alpha(\theta_{d+1})| = 0.5$. Furthermore, in the case where d is even, $\alpha_{d,\mathrm{l}} = \alpha(\theta_{d+1}) = -0.5 < 0$ and $\alpha_{d,\mathrm{u}} = \alpha(\theta_d) > 0.5 > 0$, whereas, in the case where d is odd, $\alpha_{d,\mathrm{l}} = \alpha(\theta_d) < -0.5 < 0$ and $\alpha_{d,\mathrm{u}} = \alpha(\theta_{d+1}) = 0.5 > 0$. In addition, although $\lim_{d\to\infty} \alpha(\theta_d)$ does not exist, it follows from (20) that $\lim_{d\to\infty} |\alpha(\theta_d)| = \lim_{d\to\infty} \frac{1}{\sqrt{2-2\cos\left(\frac{2d+1}{2d+3}\right)\pi}} = 0.5$, which confirms (7). For $d = 10$ and $d = 11$, Figure 5 shows $\alpha(\theta_i)$ and $|\alpha(\theta_i)|$ versus θ_i. Note that, for both values of d, the minimum value of $|\alpha(\theta_i)|$ is 0.5, which occurs at $\theta = \pi$. Finally, Figure 6 shows $\alpha_{d,\mathrm{l}}$ and $\alpha_{d,\mathrm{u}}$ versus d, which indicates that $\lim_{d\to\infty} \alpha_{d,\mathrm{l}} = -0.5$ and $\lim_{d\to\infty} \alpha_{d,\mathrm{u}} = 0.5$. ◇

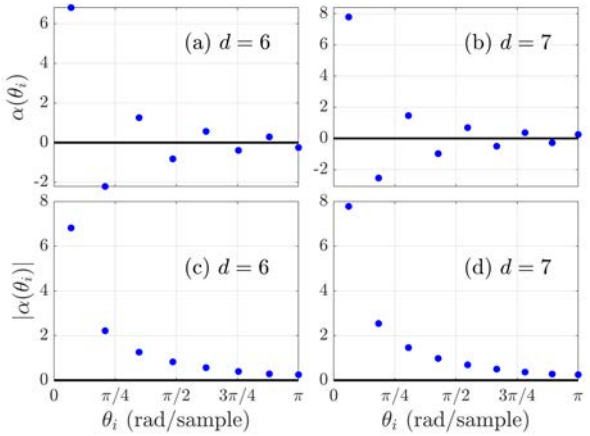

Fig. 3: Example 2.2: For $p = 0.5$, $d = 6$, and $d = 7$, (a) and (b) show $\alpha(\theta_i)$ versus θ_i, and (c) and (d) show $|\alpha(\theta_i)|$ versus θ_i. Note that the sign of $\alpha(\theta_i)$ alternates.

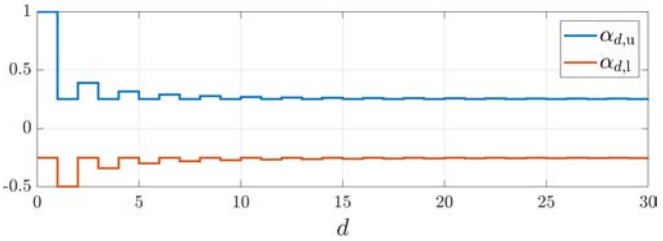

Fig. 4: Example 2.2: For $p = 0.5$, $\alpha_{d,\mathrm{l}}$ and $\alpha_{d,\mathrm{u}}$ versus d. As $d \to \infty$, $\alpha_{d,\mathrm{l}}$ and $\alpha_{d,\mathrm{u}}$ converge to $-\alpha_\infty$ and α_∞, respectively.

III. Time-Delayed Lur'e Model

Inserting the saturation nonlinearity following the washout filter G_{w} in Figure 2 yields the TDL model shown in Figure

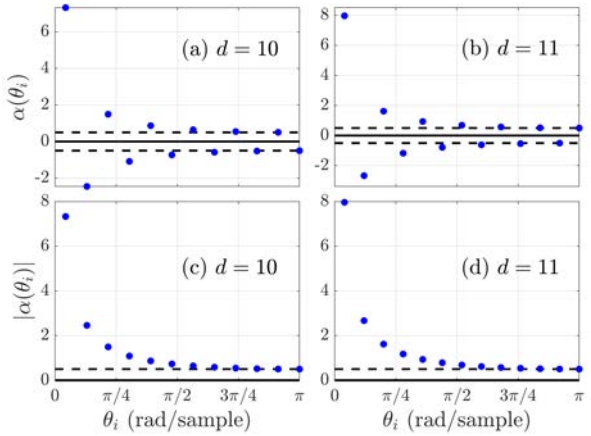

Fig. 5: Example 2.2: For $p = 0$, $d = 10$, and $d = 11$, (a) and (b) show $\alpha(\theta_i)$ versus θ_i, and (c) and (d) show $|\alpha(\theta_i)|$ versus θ_i. The dashed lines indicate $\pm\alpha_\infty$.

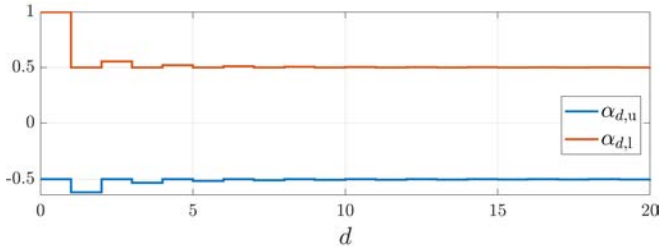

Fig. 6: Example 2.2: For $p = 0$, $\alpha_{d,\mathrm{l}}$ and $\alpha_{d,\mathrm{u}}$ versus d. As $d \to \infty$, $\alpha_{d,\mathrm{l}}$ and $\alpha_{d,\mathrm{u}}$ converge to $-\alpha_\infty$ and α_∞, respectively.

7, which has closed-loop dynamics

$$\begin{bmatrix} x_{k+1} \\ x_{\mathrm{d},k+1} \\ x_{\mathrm{w},k+1} \end{bmatrix} = \begin{bmatrix} A & 0 & 0 \\ e_{d,d}C & N_d & 0 \\ 0 & e_{1,d}^{\mathrm{T}} & 0 \end{bmatrix} \begin{bmatrix} x_k \\ x_{\mathrm{d},k} \\ x_{\mathrm{w},k} \end{bmatrix} + \begin{bmatrix} \alpha B \\ 0 \\ 0 \end{bmatrix} v_{\mathrm{f},k}, \tag{23}$$

with y_k, $y_{\mathrm{d},k}$, and $y_{\mathrm{f},k}$ given by (2), (3), and (4), respectively, where $v_{\mathrm{f},k} = \mathrm{sat}_\delta(y_{\mathrm{f},k})$ is the output of the saturation function $\mathrm{sat}_\delta \colon \mathbb{R} \to \mathbb{R}$, where $\delta > 0$, defined by

$$\mathrm{sat}_\delta(u) = \begin{cases} u, & |u| \le \delta, \\ \mathrm{sign}(u), & |u| > \delta. \end{cases} \tag{24}$$

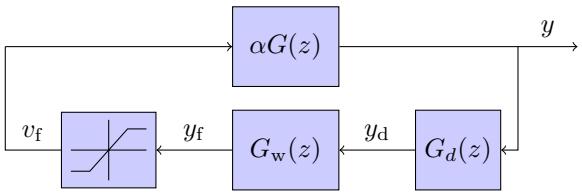

Fig. 7: Discrete-time time-delayed Lur'e model.

To analyze the self-oscillating behavior of the time-delayed Lur'e model, we replace the saturation nonlinearity by its describing function. Describing functions are used to characterize self-excited oscillations in [2, Section 5.4] as well as in [8, pp. 293–294]. The describing function $\Psi_\delta(\varepsilon)$ for sat_δ for a sinusoidal input with amplitude $\varepsilon > 0$ is given by

$$\Psi_\delta(\varepsilon) = \begin{cases} \frac{2}{\pi}\left[\sin^{-1}\left(\frac{\delta}{\varepsilon}\right) + \left(\frac{\delta}{\varepsilon}\right)\sqrt{1 - \left(\frac{\delta}{\varepsilon}\right)^2}\right], & \text{if } \varepsilon > \delta \\ 1, & \text{otherwise.} \end{cases} \tag{25}$$

Note that, for $\varepsilon > \delta$, Ψ_δ confined to (δ, ∞) with range space $(0, 1)$ is decreasing, one-to-one, and onto. Let $p_{d,\alpha,\varepsilon}$ be the characteristic polynomial of the linearized time-delay Lur'e model, such that

$$p_{d,\alpha,\varepsilon}(z) \triangleq z^{d+1}D(z) - \alpha\Psi_\delta(\varepsilon)(z-1)N(z). \tag{26}$$

For all $\varepsilon_{\mathrm{l}} > 0$, $\varepsilon_{\mathrm{u}} > 0$, $\theta_{\mathrm{l}} \in \mathbb{R}$, and $\theta_{\mathrm{u}} \in \mathbb{R}$ such that $\varepsilon_{\mathrm{l}} < \varepsilon_{\mathrm{u}}$ and $\theta_{\mathrm{l}} < \theta_{\mathrm{u}}$, define the rectangle

$$\Gamma_{\theta_{\mathrm{l}},\theta_{\mathrm{u}},\varepsilon_{\mathrm{l}},\varepsilon_{\mathrm{u}}} \triangleq \{(\theta,\varepsilon) \colon \theta_{\mathrm{l}} < \theta < \theta_{\mathrm{u}} \text{ and } \varepsilon_{\mathrm{l}} < \varepsilon < \varepsilon_{\mathrm{u}}\}$$

and the set $\Theta \triangleq \{\theta \ne 0 \colon g(\theta) = 0\}$.

Lemma 3.1: Let $\alpha \in \mathbb{R}$, and let $\theta_0 \in \Theta$ be such that $\mathrm{sign}\,\alpha_0 = \mathrm{sign}\,\alpha$ and $|\alpha_0| < |\alpha|$, where $\alpha_0 \triangleq \alpha(\theta_0)$, and let $d > \bar{d}$. Then, the following statements hold:

i) There exist $\varepsilon_0 > 0$, $\theta_{\mathrm{l}} > 0$, $\theta_{\mathrm{u}} > 0$, $\varepsilon_{\mathrm{l}} > 0$, and $\varepsilon_{\mathrm{u}} > 0$ such that $\varepsilon_{\mathrm{l}} < \varepsilon_{\mathrm{u}}$, $\theta_{\mathrm{l}} < \theta_{\mathrm{u}}$, $(\theta_0, \varepsilon_0) \in \Gamma_{\theta_{\mathrm{l}},\theta_{\mathrm{u}},\varepsilon_{\mathrm{l}},\varepsilon_{\mathrm{u}}}$, and, in the rectangle $\Gamma_{\theta_{\mathrm{l}},\theta_{\mathrm{u}},\varepsilon_{\mathrm{l}},\varepsilon_{\mathrm{u}}}$, $(\theta,\varepsilon) = (\theta_0,\varepsilon_0)$ is the unique solution of $p_{d,\alpha,\varepsilon}(e^{\jmath\theta}) = 0$.

ii)

$$\frac{\mathrm{d}}{\mathrm{d}\varepsilon}\Psi_\delta(\varepsilon)\bigg|_{\varepsilon=\varepsilon_0} \ne 0. \tag{27}$$

iii)

$$\frac{\mathrm{d}}{\mathrm{d}\theta}\mathrm{Im}[L_d(e^{\jmath\theta})]\bigg|_{\theta=\theta_0} \ne 0. \tag{28}$$

The statements of Lemma 3.1 are implied by (6) and (13).

Theorem 3.2: Consider the discrete-time time-delayed Lur'e model in Figure 7, assume that $x_0 \ne 0$, and let $\alpha \in (-\infty, \alpha_{d,\mathrm{l}}) \cup (\alpha_{d,\mathrm{u}}, \infty)$. Then, there exists a nonconstant periodic function $\tau \colon \mathbb{N} \to \mathbb{R}$ such that $\lim_{k\to\infty} |y_k - \tau_k| = 0$.

Theorem 3.2 is implied by Theorem 7.4 in [8, pp. 293, 294] and Lemma 3.1. It can be seen that Theorem 3.2 holds in the case where the saturation function is replaced by an odd sigmoidal nonlinearity such as atan or tanh.

Example 3.3: Let $G(z) = 1/z$. Figure 8 shows the transient response and asymptotic oscillatory response for $\alpha = 1.1$, $d = 0$, and $\delta = 1$ along with plot of $v_{\mathrm{f},k}$ and $y_{\mathrm{f},k}$. Figure 8(a) shows that, for $k > 80$, y_k is a nonconstant periodic function. Furthermore, Figure 8(b) shows how the saturation nonlinearity acts upon $y_{\mathrm{f},k}$, which results in the saturated signal $v_{\mathrm{f},k} \in [-\delta, \delta]$. Note how both $v_{\mathrm{f},k}$ and $y_{\mathrm{f},k}$ are also nonconstant periodic function for $k > 80$.

Figure 9 shows $\alpha(\theta_i)$ versus θ_i for $d = 0$ and $d = 1$. For $\alpha = 0.6$, only in the case $d = 1$ has $\alpha(\theta_i)$ such that $\mathrm{sign}(\alpha(\theta_{\mathrm{i}})) = \mathrm{sign}(\alpha)$ and $|\alpha(\theta_i)| < |\alpha|$. For $\alpha = 1.1$, both models meet the conditions for α.

Figure 10 shows the response of y_k for $\delta = 1$ and all possible pairs of $d = 0, 1$ and $\alpha = 0.6, 1.1$. For $\alpha = 0.6$, only

the model with $d = 1$ yields a limit cycle. For $\alpha = 1.1$, both models yield oscillations. This follows from the conditions for α stated in the previous paragraph and in lemma 3.1.

Finally, Figure 11 shows the magnitude of the frequency response for models with $\alpha = 1.1$, $\delta = 1$, and $d = 0, 1$. Note that the frequencies corresponding to the magnitude peaks are similar to the values of θ_i shown in Figure 9 such that $\text{sign}(\alpha(\theta_i)) = \text{sign}(\alpha)$ and $|\alpha(\theta_i)| < |\alpha|$. ◇

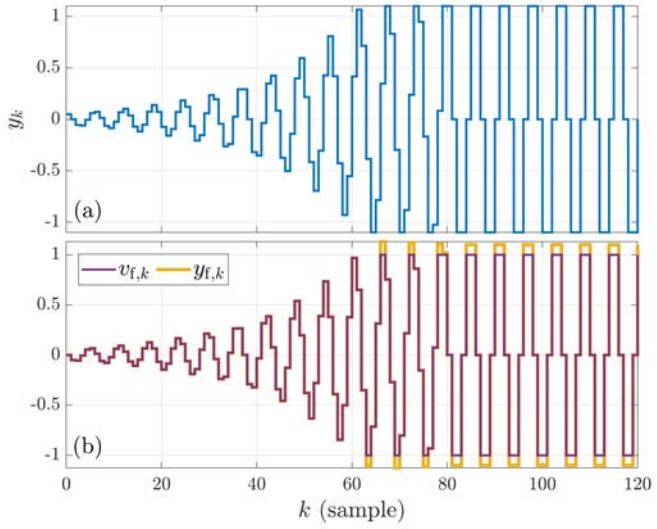

Fig. 8: Example 3.3: For $d = 0$, $\delta = 1$, and $\alpha = 1.1$, (a) shows y_k, and (b) shows $v_{\mathrm{f},k}$ and $y_{\mathrm{f},k}$. The saturation nonlinearity, with $\delta = 1$, saturates the values of $y_{\mathrm{f},k}$, resulting in $v_{\mathrm{f},k} \in [-\delta, \delta]$.

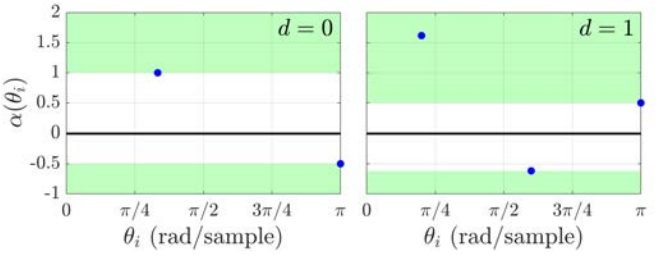

Fig. 9: Example 3.3: For $d = 0$ and $d = 1$, these plots show the values $\alpha(\theta_i)$ of α for which the closed-loop dynamics have a pole on the unit circle at the angle θ_i for $i = 1, \ldots, d + 2$. For the case $d = 0$, where $\theta_1 = 1.0472$ and $\theta_2 = \pi$, the time-delayed Lur'e model has self-excited oscillations if and only if either $\alpha > 1$ or $\alpha < -0.5$, while, for the case $d = 1$, where $\theta_1 = 0.6283$, $\theta_2 = 1.8850$ and $\theta_3 = \pi$, the TDL model has self-excited oscillations if and only if either $\alpha > 0.5$ or $\alpha < -0.618$. For all values of α corresponding to the shaded regions, the response of the TDL model oscillates.

IV. Time-Delayed Lur'e Model with Bias Generation

We now modify the discrete-time time-delay Lur'e model by including the bias-generation mechanism shown in Figure 1. The corresponding closed-loop dynamics are thus given by

$$\begin{bmatrix} x_{k+1} \\ x_{\mathrm{d},k+1} \\ x_{\mathrm{w},k+1} \end{bmatrix} = \begin{bmatrix} A & 0 & 0 \\ e_{d,d}C & N_d & 0 \\ 0 & e_{1,d}^{\mathrm{T}} & 0 \end{bmatrix} \begin{bmatrix} x_k \\ x_{\mathrm{d},k} \\ x_{\mathrm{w},k} \end{bmatrix} + \begin{bmatrix} B \\ 0 \\ 0 \end{bmatrix} v_{\mathrm{b},k}, \quad (29)$$

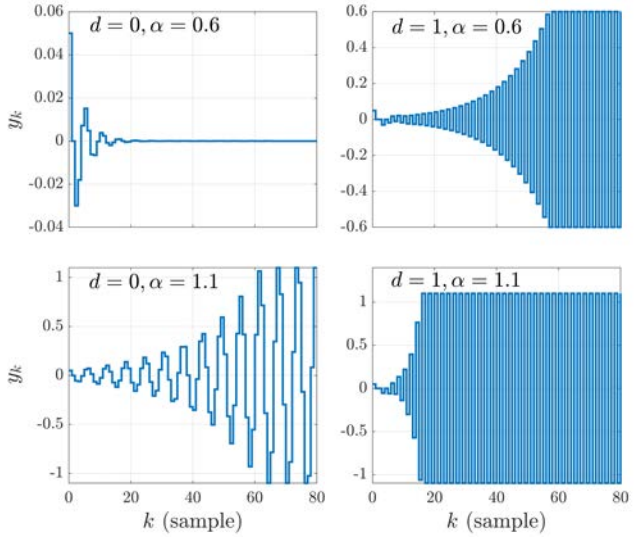

Fig. 10: Example 3.3: Response y_k of the TDL model for $d = 0, 1$ and $\alpha = 0.6, 1.1$ with $\delta = 1$.

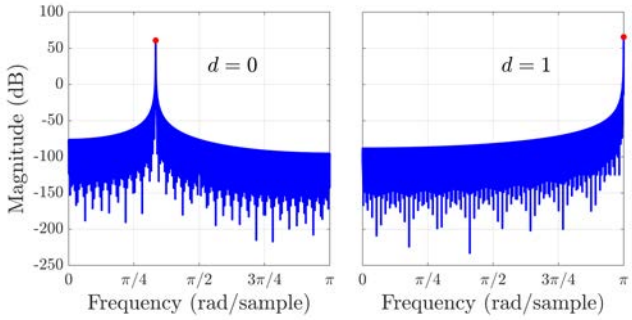

Fig. 11: Example 3.3: Frequency response of y_k for $d = 0, 1$ with $\alpha = 1.1$ and $\delta = 1$. Note that, for $d = 0$, the peak is located at θ_1, whereas, for $d = 1$, the peak is located at θ_3.

with y_k, $y_{\mathrm{d},k}$, and $y_{\mathrm{f},k}$ given by (2), (3), and (4), respectively, where β is a constant,

$$v_{\mathrm{b},k} = (\beta + v_{\mathrm{f},k})v_k, \quad (30)$$

and $v_{\mathrm{f},k} = \text{sat}_\delta(y_{\mathrm{f},k})$. Note that the constant α is now omitted. Instead, the constant input v is injected multiplicatively inside the loop, thus playing the role of α. This feature allows the offset of the oscillation to depend on the external input. The resulting bias $\bar{y}$ of the periodic response is thus given by

$$\bar{y} = v\beta G(1). \quad (31)$$

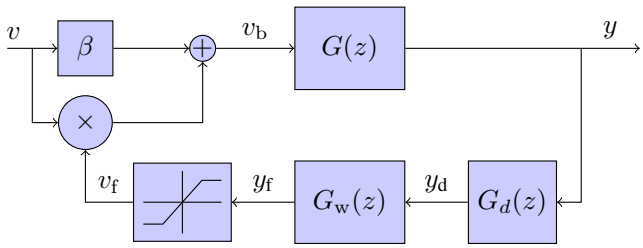

Fig. 12: Discrete-time time-delayed Lur'e model with constant input v and bias generation.

Example 4.1: Let $G(z) = 1/z$, $d = 0$, $\beta = 2.5$, $v = 1.1$, and $\delta = 1$. Figure 13(a) shows that the output y_k is oscillatory with offset $\bar{y} = v\beta G(1) = 2.75$. Figure 13(b) shows $v_{\mathrm{f},k}$ and $y_{\mathrm{f},k}$. Note that, as in Example 3.3, despite the offset $\bar{y}$ of y_k, the signals $y_{\mathrm{f},k}$ and $v_{\mathrm{f},k}$ oscillate without an offset. Finally, Figure 13(c) shows the magnitude of the frequency response for $y_k - \bar{y}$. Note that the peak is located near the same frequency as in Example 3.3, and thus the oscillation frequency remains the same with the addition of the bias-generation mechanism. ◇

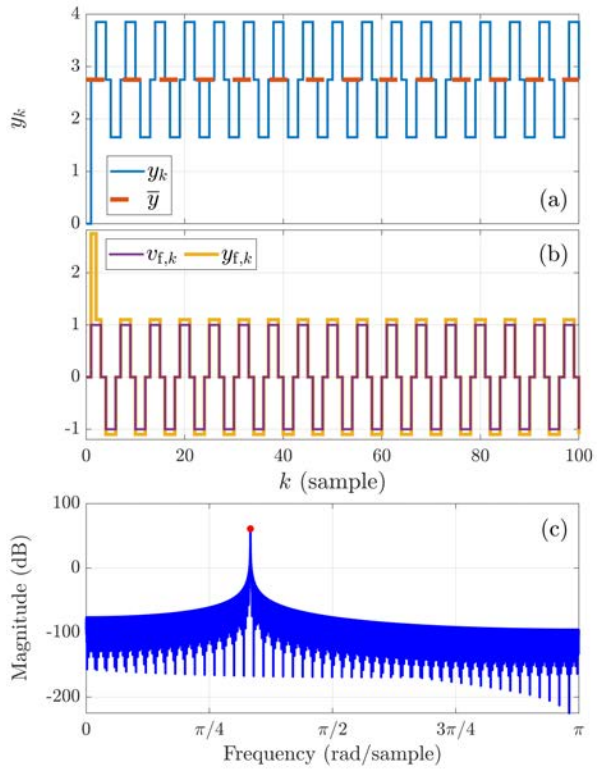

Fig. 13: Example 4.1: For $v = 1.1$, $\beta = 2.5$, $d = 0$, and $\delta = 1$, (a) shows y_k and the offset $\bar{y}$, (b) shows $v_{\mathrm{f},k}$ and $y_{\mathrm{f},k}$, and (c) shows the frequency response of $y_k - \bar{y}$.

V. Conclusions

This paper presented and analyzed a discrete-time Lur'e model that exhibits self oscillation. This model involves an arbitrary asymptotically stable linear system, a time delay, a washout filter, and a saturation nonlinearity. It was shown that, for sufficiently large loop gain, the response converges to a periodic signal, and thus the system has self-excited oscillations. This result can be extended to sigmoidal nonlinearities described by *iv*) in Section I. A bias-generation mechanism provides an input-dependent oscillation offset. The amplitude and spectral content of the oscillation were analyzed in terms of the components of the model. Future work will include a more detailed analysis of the discrete-time self-excited model and use it for system identification and adaptive stabilization.

VI. Acknowledgments

This research was supported by NSF grant CMMI 1634709, "A Diagnostic Modeling Methodology for Dual Retrospective Cost Adaptive Control of Complex Systems."

References

[1] A. Jenkins, "Self-oscillation," *Physics Reports*, vol. 525, no. 2, pp. 167–222, 2013.
[2] W. Ding, *Self-Excited Vibration: Theory, Paradigms, and Research Methods*. Springer, 2010.
[3] B. Chance, E. K. Pye, A. K. Ghosh, and B. Hess, Eds., *Biological and Biochemical Oscillators*. Academic Press, 1973.
[4] P. Gray and S. K. Scott, *Chemical Oscillations and Instabilities: Nonlinear Chemical Kinetics*. Oxford, 1990.
[5] A. Goldbeter and M. J. Berridge, *Biochemical Oscillations and Cellular Rhythms: The Molecular Bases of Periodic and Chaotic Behaviour*. Cambridge, 1996.
[6] Y. Chen and J. F. Driscoll, "A multi-chamber model of combustion instabilities and its assessment using kilohertz laser diagnostics in a gas turbine model combustor," *Combustion and Flame*, vol. 174, pp. 120–137, 2016.
[7] E. Awad and F. E. C. Culick, "On the existence and stability of limit cycles for longitudinal acoustic modes in a combustion chamber," *Combustion Science and Technology*, vol. 46, pp. 195–222, 1986.
[8] H. K. Khalil, *Nonlinear Systems*, 3rd ed. Prentice Hall, 2002.
[9] X. Jian and C. Yu-shu, "Effects of time delayed velocity feedbacks on self-sustained oscillator with excitation," *Applied Mathematics and Mechanics*, vol. 25, no. 5, pp. 499–512, May 2004.
[10] D. H. Zanette, "Self-sustained oscillations with delayed velocity feedback," *Papers in Physics*, vol. 9, pp. 090 003–1–090 003–7, March 2017.
[11] S. Risau-Gusman, "Effects of time-delayed feedback on the properties of self-sustained oscillators," *Phys. Rev. E*, vol. 94, p. 042212, October 2016.
[12] S. Chatterjee, "Self-excited oscillation under nonlinear feedback with time-delay," *Journal of Sound and Vibration*, vol. 330, no. 9, pp. 1860–1876, 2011.
[13] G. Stan and R. Sepulchre, "Analysis of interconnected oscillators by dissipativity theory," *IEEE Transactions on Automatic Control*, vol. 52, no. 2, pp. 256–270, 2007.
[14] E. A. Tomberg and V. A. Yakubovich, "Conditions for auto-oscillations in nonlinear systems," *Siberian Mathematical Journal*, vol. 30, no. 4, pp. 641–653, 1989.
[15] A. Mees and L. Chua, "The hopf bifurcation theorem and its applications to nonlinear oscillations in circuits and systems," *IEEE Transactions on Circuits and Systems*, vol. 26, no. 4, pp. 235–254, 1979.
[16] S. M. Savaresi, R. R. Bitmead, and W. J. Dunstan, "Non-linear system identification using closed-loop data with no external excitation: The case of a lean combustion chamber," *International Journal of Control*, vol. 74, no. 18, pp. 1796–1806, 2001.
[17] V. Rasvan, "Self-sustained oscillations in discrete-time nonlinear feedback systems," in *Proc. 9th Mediterranean Electrotechnical Conference*, 1998, pp. 563–565.
[18] M. B. D'Amico, J. L. Moiola, and E. E. Paolini, "Hopf bifurcation for maps: a frequency-domain approach," *IEEE Transactions on Circuits and Systems I: Fundamental Theory and Applications*, vol. 49, no. 3, pp. 281–288, March 2002.
[19] D'Amico, M. Belen, J. L. Motola, and E. E. Paolini, "Study of degenerate bifurcations in maps: A feedback systems approach," *International Journal of Bifurcation and Chaos*, vol. 14, no. 05, pp. 1625–1641, 2004.
[20] F. S. Gentile, A. L. Bel, M. Belén D'Amico, and J. L. Moiola, "Effect of delayed feedback on the dynamics of a scalar map via a frequency-domain approach," *Chaos: An Interdisciplinary Journal of Nonlinear Science*, vol. 21, no. 2, p. 023117, 2011.
[21] N. Minorsky, "Self-excited oscillations in dynamical systems possessing retarded actions," in *Classic Papers in Control Theory*, R. Bellman and R. Kalaba, Eds. Dover, 2010, pp. 143–149.
[22] G. Stan and R. Sepulchre, "Global analysis of limit cycles in networks of oscillators," *IFAC Proceedings Volumes*, vol. 37, no. 13, pp. 1153–1158, 2004, 6th IFAC Symposium on Nonlinear Control Systems.
[23] M. A. Hassouneh, H.-C. Lee, and E. H. Abed, "Washout filters in feedback control: Benefits, limitations and extensions," in *Proc. Amer. Contr. Conf.*, Boston, June/July 2004, pp. 3950–3955.